Method to determine the optimal impedance profile of nonuniform transmission lines used for pulsed power accelerators

Quan Zhou,[1] Xinlei Zhu,[2,*] and Yaping Du[1]

[1]*Department of Building Energy and Environment Engineering, The Hong Kong Polytechnic University, Hong Kong, China*

[2]*Sichuan Energy Internet Research Institute, Tsinghua University, Chengdu, China*

(Received 24 April 2024; accepted 10 July 2024; published 5 August 2024)

Nonuniform transmission lines (NTLs) are widely used in pulsed power accelerators because they provide an efficient way to achieve impedance matching and pulse shaping. Since designing and constructing these accelerators typically demands substantial effort, finding the optimal impedance profile to maximize the power transmission efficiencies of the NTLs is important. In this paper, a convenient numerical method to determine the optimal impedance profile is proposed. First, the output of the NTL with arbitrary parameters is theoretically analyzed under arbitrary input conditions. It was found that only four factors affect the power transmission efficiency: the ratio of output impedance to input impedance, the ratio of input pulse width to the NTL's one-way transit time, the normalized impedance profile, and the normalized input pulse. Based on these findings, a method designed to minimize the reflected component within the working frequency range is proposed. Using this method, an impedance profile demonstrating superior power transmission efficiency compared to the traditional exponential profile is identified. This work can provide a rapid and effective method to determine the impedance profile of the NTL, undoubtedly benefiting the design process of pulsed power accelerators.

DOI: 10.1103/PhysRevAccelBeams.27.080401

I. INTRODUCTION

Nonuniform transmission lines (NTLs) are an efficient way to achieve impedance matching and pulse shaping, and are therefore, widely used in pulsed power accelerators, such as high-gradient particle accelerators [1] and Z-pinch accelerators [2–6]. For example, in the recently published designs of petawatt-class Z-pinch accelerators [2–4], the monolithic water-insulated radial transmission line used to combine and transmit the outputs of several hundred generators is a type of NTL.

Among various impedance profiles, the exponential nonuniform transmission line (ENTL) is frequently selected for its superior transmission efficiency [2–4,7–10]. Zhang *et al.* adopted the circuit simulation and demonstrated that the ENTL has a higher power efficiency than the Gaussian NTL [7]. Similarly, Hu *et al.* proposed that the ENTL has higher power efficiencies than the Gaussian and linear NTLs [8]. However, Welch *et al.* investigated some specific cases and found that the optimal impedance profile gradually deviates from an exponential form as the pulse width to one-way transit time ratio increases from zero [9].

Most of the previous researches on the optimal impedance profile employed circuit simulations to evaluate the power transmission efficiency of various impedance profiles, given predefined NTL parameters, that is, input impedance, output impedance, and one-way transit time. Although a numerical approach to determine the optimal impedance profile for specific input pulse shape and width has been introduced [9], this method fundamentally relies on an exhaustive search. The precision of this approach depends on the number of discrete elements used and the initial impedance profile selection. Achieving an accurate optimal impedance profile necessitates a substantial number of discrete elements, which can significantly increase computational efforts. Given the extensive design and construction efforts required for future petawatt-class pulsed-power accelerators, enhancing our understanding of NTLs and developing effective strategies to find the optimal impedance profile is crucial.

In this paper, the transmission characteristics of NTLs are analyzed and a rapid and effective method to determine the optimal impedance profile is proposed. In Sec. II, the output of NTLs under varying input conditions and arbitrary parameters is theoretically analyzed. The method to find the optimal impedance profile is put forward and verified in Sec. III. The conclusion is presented in Sec. IV.

[*]Contact author: ibelieve112358@126.com

II. TRANSMISSION CHARACTERISTICS OF NTL

Figure 1 illustrates a schematic of a variable impedance profile $Z(x)$ of the NTL and an arbitrary input voltage pulse $U_{\text{in}}(t)$. The input impedance is Z_{in} at $x = 0$, and the output impedance is Z_{out} at $x = L$. The pulse width of the input pulse is T. To investigate the transmission characteristics of the NTL, it is assumed that both the input and output are connected to a matched constant-impedance transmission line.

To streamline the analysis, both the impedance profile and the input pulse are normalized as per Eqs. (1) and (2). The corresponding schematic representations are depicted in Fig. 2:

$$\bar{Z}(\bar{x}) = \frac{Z(\bar{x}L) - Z_{\text{in}}}{Z_{\text{out}} - Z_{\text{in}}}, \tag{1}$$

$$\bar{U}_{\text{in}}(\bar{t}) = U_{\text{in}}(\bar{t}T). \tag{2}$$

The transmission characteristics of the NTL are analyzed in the frequency domain. For frequency analysis, the input voltage is a continuous sine wave, which can be represented as $A\mathrm{e}^{\mathrm{j}\omega t}$ in phasor, where A denotes the amplitude and ω denotes the angular frequency. For the NTL, the one-way transit time is T_{line} and the root mean square of $Z_{\text{out}}/Z_{\text{in}}$ is denoted as ρ_0. Due to impedance variation in the NTL, the input voltage will undergo both transmission and reflection when transmitting, as previously described in Refs. [11–13]. The components that have undergone an odd number of reflections will arrive at the inlet of the NTL, consisting of the reflected voltage. The components that have undergone an even number of reflections will arrive at the outlet of the NTL, consisting of the output voltage. Given that the optimization aims to increase the output voltage, the components that make up the output voltage are discussed in this section. The frequency response of the components contributing to the output voltage is presented in Appendix A. All the components are the functions of ρ_0, $\bar{Z}(\bar{x})$ and T_{line}.

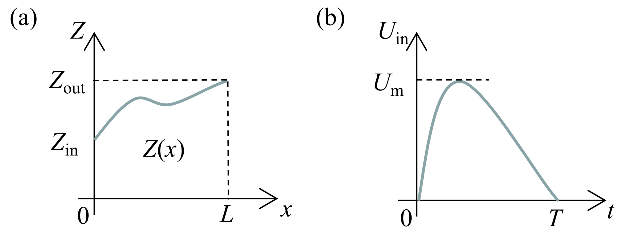

FIG. 1. Schematic of the impedance profile of the NTL (a) and the input pulse (b).

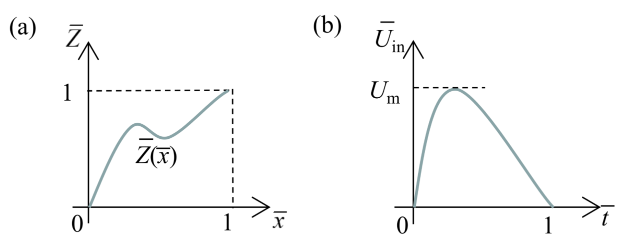

FIG. 2. Schematic of the normalized impedance profile of the NTL (a) and the normalized input pulse (b).

For an arbitrary input voltage pulse $U_{\text{in}}(t)$, its Fourier spectrum is

$$F_{\text{in}}(\omega) = \int_0^T U_{\text{in}}(t)\mathrm{e}^{-\mathrm{j}\omega t}\mathrm{d}t = T\int_0^1 \bar{U}_{\text{in}}(\bar{t})\mathrm{e}^{-\mathrm{j}\omega\bar{t}T}\mathrm{d}\bar{t}. \tag{3}$$

As observed, $F_{\text{in}}(\omega)$ is a function of $\bar{U}_{\text{in}}(\bar{t})$ and T. Considering that the spectrum of the output pulse is derived from the multiplication of the input pulse's spectrum and the frequency response, the output pulse is determined by ρ_0, $\bar{Z}(\bar{x})$, T_{line}, $\bar{U}_{\text{in}}(\bar{t})$, and T.

Further analysis reveals that the effects of T and T_{line} on the normalized output pulse are interconnected. Specifically, maintaining a constant T/T_{line}, the output pulse normalized in time is constant. An illustration of this concept is provided by considering the output component that has been reflected twice, where its frequency response is

$$F_{\text{out},N=2}(\omega) = H_{\text{out2}}(\omega)F_{\text{in}}(\omega). \tag{4}$$

It is straightforward to demonstrate that when both T and T_{line} are scaled up by a factor of n, there exists a relationship where

$$F_{\text{out},N=2}(\omega, nT, nT_{\text{line}}) = nF_{\text{out},N=2}(n\omega, T, T_{\text{line}}). \tag{5}$$

The time domain waveform of this component can be calculated from the Fourier inverse transform, and there exists

$$U_{\text{out},N=2}(t, nT, nT_{\text{line}}) = U_{\text{out},N=2}(t/n, T, T_{\text{line}}). \tag{6}$$

It can be seen that when both T and T_{line} are scaled by a factor of n, the shape of this output component remains the same, while its width increases proportionally by n. This conclusion similarly applies to other components, confirming that the normalized output pulse remains constant when the T/T_{line} ratio is preserved. Therefore, the normalized output pulse is the function of only four parameters and they are ρ_0, $\bar{Z}(\bar{x})$, $\bar{U}_{\text{in}}(\bar{t})$, and T/T_{line}.

Following precedents set in Refs. [7–9], the optimization criterion for the impedance profile is chosen to be the power transmission efficiency. Since the efficiency is only related to the ratio between the normalized input and output pulses, four factors affect the power transmission efficiency and they are ρ_0, $\bar{Z}(\bar{x})$, T/T_{line}, and $\bar{U}_{\text{in}}(\bar{t})$. Taking an ENTL and a half-sine input wave as an example, the power transmission efficiency as a function of ρ_0 and T/T_{line} is

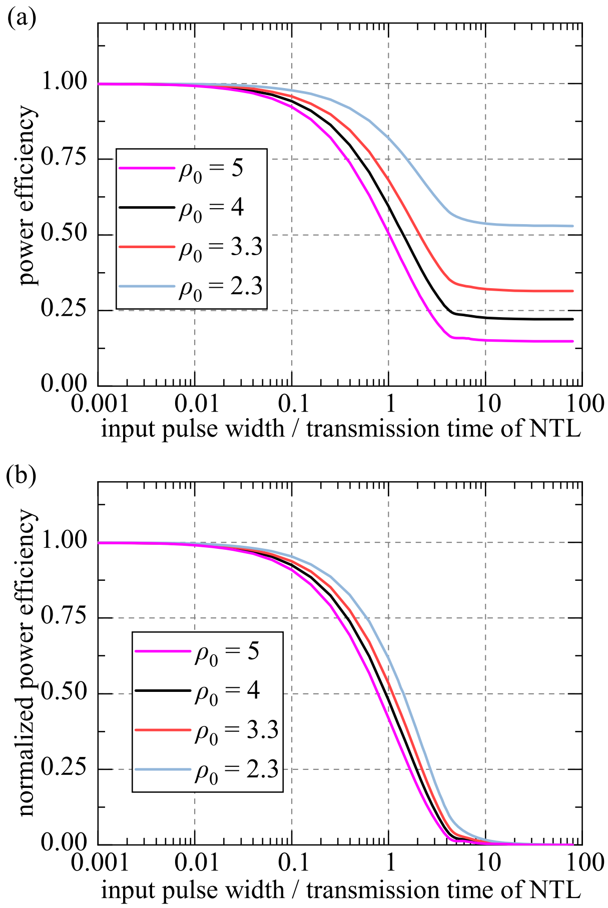

FIG. 3. Power transmission efficiency (a) and normalized power transmission efficiency (b) as a function of ρ_0 and T/T_{line} for an ENTL and a half-sine input wave.

shown in Fig. 3. In the long-pulse limit, that is, $T/T_{\mathrm{line}} \to \infty$, the power transmission efficiency converges toward the low-frequency result.

III. METHOD TO OPTIMIZE IMPEDANCE PROFILE

Section II analyzes the factors influencing power transmission efficiency. Given that the input impedance and output impedance are determined by the pulse source and load, respectively, the value of ρ_0 is typically predetermined at the design stage. Consequently, this paper aims to optimize the normalized impedance profile $\bar{Z}(\bar{x})$ under various conditions of ρ_0, T/T_{line}, and $\bar{U}_{\mathrm{in}}(\bar{t})$.

Although deriving a general analytical expression for the optimal impedance profile may be unfeasible, a convenient numerical method is proposed in this paper. This method primarily aims to minimize the reflected component within the working frequency range of the NTL. As the NTL functions as a linear passive two-port network, reducing the reflected component inherently boosts the output component and, subsequently, enhances power transmission efficiency. Previous studies have shown that the component reflected once predominantly constitutes the reflected pulse in pulsed power applications [11–14]; thus the analysis will focus solely on this component.

This section is divided into two parts: the first details the numerical method, and the second presents a case study to demonstrate its efficacy.

A. Method introduction

For the component reflected once, its frequency response is

$$\Gamma_1(\omega) = \int_0^L \frac{\mathrm{d}(\ln(Z(x)))}{2\mathrm{d}x} \mathrm{e}^{-\mathrm{j}\omega T_{\mathrm{line}} 2x/L}. \quad (7)$$

For simplicity, $\mathrm{d}(\ln(Z(x)))/(2\mathrm{d}x)$ is denoted as $N(x)$, and the relationship between $Z(x)$ and $N(x)$ is

$$Z(x) = \mathrm{e}^{\int 2N(x)}. \quad (8)$$

The objective function of this method is to minimize the integral of the reflected component over the working frequency range. Since the spectrum of the input pulse varies across different frequencies, this spectrum is incorporated as a weighting factor in the optimization process. Consequently, the objective function is defined as the weighted integral of the squared magnitude of the reflected component, effectively prioritizing frequencies where the input pulse has higher spectral content. The objective function is shown in Eq. (9). ω_1 and ω_2 are the minimum and maximum frequencies of the working frequency range of the NTL, respectively, and $W(\omega)$ is the magnitude of the input pulse spectrum.

The function $N(x)$, which is directly influenced by the impedance profile $Z(x)$, is the target of our optimization strategy. To facilitate the optimization, $N(x)$ is expressed as a polynomial function using Taylor expansion, where the polynomial is defined up to a maximum order of k, as shown in Eq. (10). By solving for $N(x)$, we effectively seek to minimize the objective function, optimizing the impedance profile for enhanced transmission efficiency:

$$\begin{aligned} P_{\mathrm{ref1}} &= \int_{\omega_1}^{\omega_2} |\Gamma_1(\omega)|^2 W(\omega)\mathrm{d}\omega \\ &= \int_0^L \int_0^L N(x)N(x') \\ &\quad \times \int_{\omega_1}^{\omega_2} W(\omega)\cos(2\omega T_{\mathrm{line}}(x'-x)/L)\mathrm{d}\omega\mathrm{d}x\mathrm{d}x', \end{aligned} \quad (9)$$

$$N(x) = \sum_{i=0}^{k} a_i x^i. \quad (10)$$

By solving for the coefficients a_i, the expression for $N(x)$ is derived, and then $Z(x)$ can be determined. It is crucial that k, the maximum order of expansion, is sufficiently large to encompass a comprehensive range of impedance profiles. By substituting Eq. (10) into Eq. (9), we have

$$P_{\mathrm{ref1}} = \sum_{i=0}^{k}\sum_{j=0}^{k} a_i a_j f(i,j), \tag{11}$$

where

$$f(i,j) = \int_0^L \int_0^L \int_{\omega_1}^{\omega_2} x^i x'^j W(\omega)\cos(2\omega T_{\mathrm{line}}(x'-x)/L) \times \mathrm{d}\omega \mathrm{d}x \mathrm{d}x'. \tag{12}$$

Those coefficients a_i ($i = 0, 1, 2, ..., k$) are not independent of each other, and only the coefficients a_i ($i = 1, 2, ..., k$) need to be solved. Taking this limitation into consideration, the expression of P_{ref1} is presented in Appendix B. To minimize P_{ref1}, P_{ref1} performs partial differentiation on each unknown quantity a_i and sets the result to zero, as shown in Appendix B. Finally, a matrix equation can be obtained

$$\begin{bmatrix} A(1,1) & A(1,2) & \cdots & A(1,k) \\ A(2,1) & A(2,2) & & \vdots \\ \vdots & & \ddots & \vdots \\ A(k,1) & \cdots & \cdots & A(k,k) \end{bmatrix} \begin{bmatrix} a_1 \\ a_2 \\ \vdots \\ a_k \end{bmatrix} = \begin{bmatrix} B(1) \\ B(2) \\ \vdots \\ B(k) \end{bmatrix}, \tag{13}$$

where

$$\begin{cases} A(i,n) = \frac{2L^{i+n} f(0,0)}{(i+1)(n+1)} - \frac{2L^i}{i+1} f(0,n) - \frac{2L^n}{n+1} f(0,i) + 2f(i,n) \\ B(n) = \frac{1}{L}\ln\frac{Z_{\mathrm{out}}}{Z_{\mathrm{in}}}\left(\frac{L^n}{n+1} f(0,0) - f(0,n)\right) \end{cases}. \tag{14}$$

By solving this matrix equation, those coefficients a_i can be calculated, and hence $Z(x)$ is obtained using the below equation:

$$Z(x) = Z_{\mathrm{in}} \exp\left[\ln\frac{Z_{\mathrm{out}}}{Z_{\mathrm{in}}} + \sum_{n=1}^{k} \frac{2a_n}{n+1}\left(x^{n+1} - L^{n+1}\right)\right]. \tag{15}$$

In summary, the method for optimizing the impedance profile is structured into four sequential steps: (i) perform the Fourier transform on the input pulse and calculate the amplitude of its spectrum, that is, $W(\omega)$; (ii) set an initial value for k and utilize Eqs. (12) and (14) to derive Eq. (13). Solving Eq. (13) allows for the determination of the coefficients a_i: (iii) substitute those coefficients into Eq. (15) to calculate the impedance profile $Z(x)$; (iv) increase the value of k and repeat steps 2 and 3. If changes in $Z(x)$ are negligible, consider $Z(x)$ as the optimal impedance profile. If there is a non-negligible change in $Z(x)$, increase k and continue the iterative process. A detailed visualization of this procedure is provided in Fig. 4.

B. Method verification

In this part, a case study is used to verify the effectiveness of the proposed method.

For the pulsed power application, the input pulse is usually similar to a half-sine wave with the following expression:

$$V_{\mathrm{in}}(t) = \begin{cases} 0 & t \le 0 \\ V_0 \sin(\omega_0 t) & 0 \le t \le \frac{\pi}{\omega_0} \\ 0 & t \ge \frac{\pi}{\omega_0} \end{cases}, \tag{16}$$

where V_0 is the peak of the input pulse, and ω_0 determines the pulse width T according to $T = \pi/\omega_0$.

According to the Fourier transform, the spectrum of this input pulse is

$$F(\omega) = \int_0^T \sin(\pi t/T)\mathrm{e}^{-\mathrm{j}\omega t} dt = \frac{2T\pi \mathrm{e}^{-\mathrm{j}T\omega/2}\cos(T\omega/2)}{-T^2\omega^2 + \pi^2}. \tag{17}$$

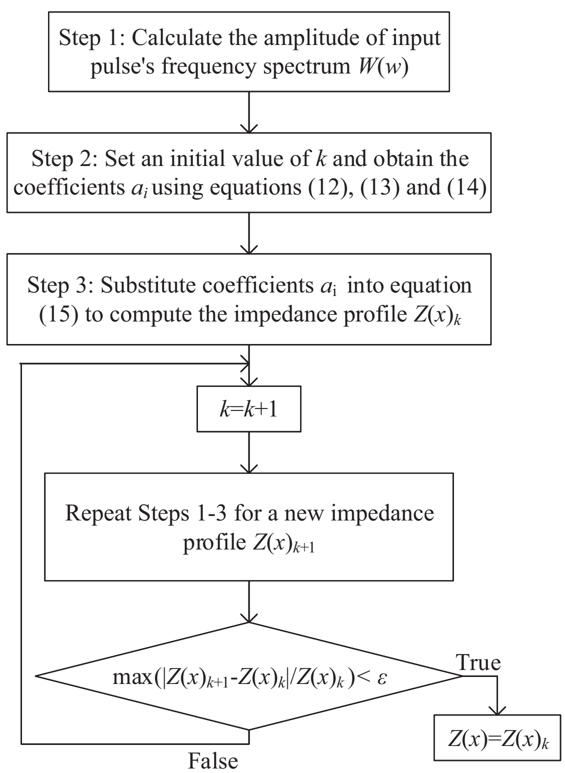

FIG. 4. Flowchart of the process to obtain the optimal impedance profile.

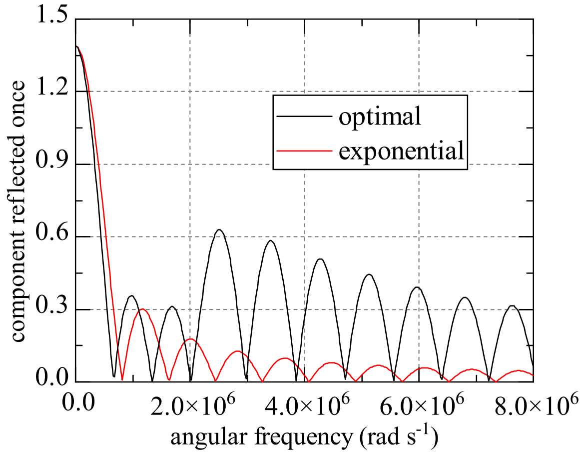

FIG. 5. Schematic of the weight function $W(\omega)$.

The weight function $W(\omega)$ is the magnitude of $F(\omega)$, and it is

$$W(\omega) = \left| \frac{2T\pi \cos(T\omega/2)}{-T^2\omega^2 + \pi^2} \right|. \tag{18}$$

As shown in Fig. 5, when the angular frequency increases, the value of the weight function changes in a wavy pattern, and the peak of the wave gradually decreases to zero. Considering this characteristic, when computing Eq. (12), the lower limit of the integral ω_1 is 0, and the upper limit of the integral ω_2 is chosen as $26\omega_0$ in this paper.

As demonstrated in the last section, the parameters influencing power transmission efficiency include ρ_0, $\bar{Z}(\bar{x})$, T/T_{line} and $\bar{U}_{\mathrm{in}}(\bar{t})$. Given that $\bar{U}_{\mathrm{in}}(\bar{t})$ is predefined as Eq. (16), the factors affecting the impedance profile are reduced to ρ_0 and T/T_{line}. To verify the proposed method, the NTL design detailed in Ref. [2] is considered. Its parameters are $Z_{\mathrm{out}}/Z_{\mathrm{in}} = 16.05$ and $L = 2063$ cm, which corresponds to $\rho_0 = 4.006$ and $T_{\mathrm{line}} = 615$ ns for a water-filled line. Since ρ_0 is fixed, the power transmission efficiency is only determined by T/T_{line}. Calculations were performed to obtain the optimal impedance profile for various T/T_{line}. Results are presented in Fig. 6. For comparison, the power transmission efficiency of the exponential impedance profile is also displayed.

As we can see, the power transmission efficiency approaches 100% in the short-pulse limit (as $T/T_{\mathrm{line}} \to 0$) and approaches the low-frequency result (as $T/T_{\mathrm{line}} \to \infty$) in the long-pulse limit, regardless of the impedance profile. In addition, the optimal impedance profile deviates from an exponential form for input pulses with $T/T_{\mathrm{line}} > 0.5$, which is the same as the results in Ref. [9]. However, unlike in Ref. [9], where the power transmission efficiency difference between optimal and exponential profiles for T/T_{line} ranging from 0.5 to 1 is less than 1%, the result in this paper presents a larger efficiency gain. Specifically, at $T/T_{\mathrm{line}} = 1$, the efficiency difference is found to be 3.83%. Figures 7 and 8 illustrate the optimal and exponential impedance profiles, along with the waveforms of the input and output pulses for both profiles at $T/T_{\mathrm{line}} = 1$, showcasing the improvements achieved in this paper.

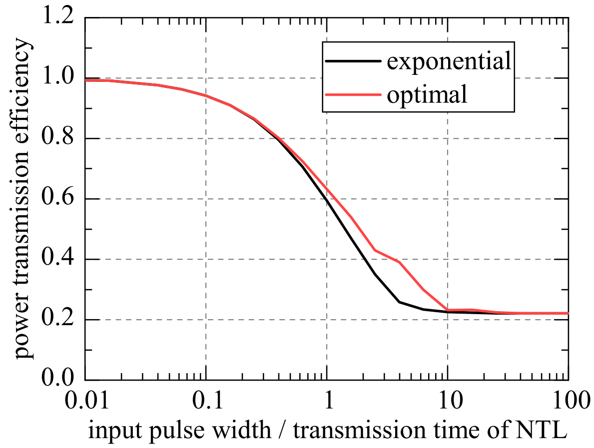

FIG. 6. Power transmission efficiency as a function of T/T_{line} for the exponential and optimal impedance profiles.

To demonstrate the power transfer efficiency predicted by the proposed method, a circuit simulation was conducted using CST DS, a commercial circuit simulation software. The optimal NTL is divided into 301 equal-length segments. Each segment is replaced by a uniform transmission line whose impedance is taken as the average of the impedances of the segments. In order to avoid interference from reflected waves, a 200 m uniform transmission line whose impedance is the input impedance of the NTL is added between the half-sine voltage source and the NTL. After removing the transmission time of the 200 m uniform transmission line, the output voltage obtained from the CST simulation and the code in our manuscript is compared in Fig. 9. As we can see, they are almost the same.

The improvement in efficiency can be explained through frequency domain analysis. Figure 10 illustrates a

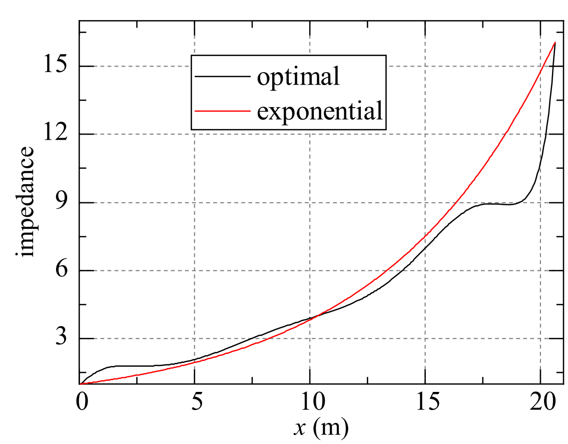

FIG. 7. Optimal and exponential impedance profiles at $T/T_{\mathrm{line}} = 1$.

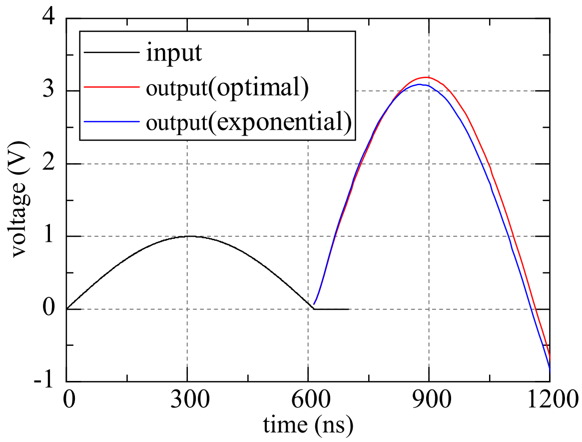

FIG. 8. Input pulse and output pulses for the optimal and exponential impedance profiles at $T/T_{\mathrm{line}} = 1$.

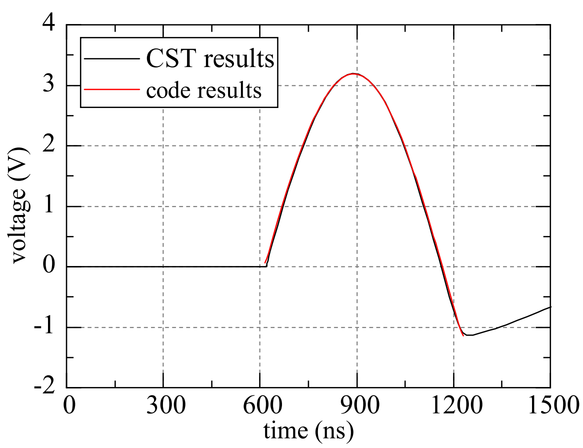

FIG. 9. Comparison of results obtained from CST simulation software and the code.

comparison of the component reflected once for both the optimal and exponential impedance profiles at $T/T_{\mathrm{line}} = 1$. The reflection component of the NTL is predominantly due to the component reflected once; thus a smaller once-reflected component correlates with higher transmission efficiency. According to Fig. 10, the optimal impedance profile does not outperform the exponential one across all frequency bands. In the low-frequency band, the optimal profile exhibits higher transmission efficiency than the exponential profile, whereas in the high-frequency band, it performs less effectively. This suggests that the optimal impedance profile sacrifices some high-frequency characteristics to enhance low-frequency transmission efficiency. Given that the spectrum of the input pulse primarily resides in the low-frequency band, as shown in Fig. 5, the power transmission efficiency of the optimal profile surpasses that of the exponential one. Similarly, the explanation of Fig. 6 can be linked to these results in Fig. 10. As T/T_{line} increases,

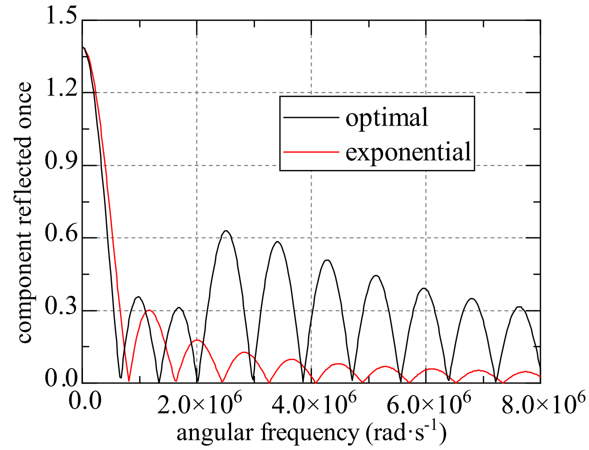

FIG. 10. Amplitude of the component reflected once in the frequency domain for the optimal and exponential impedance profiles at $T/T_{\mathrm{line}} = 1$.

the input pulse's spectrum increasingly dominates the low-frequency band, making the optimal result more effective.

As shown in the above case, the optimal impedance profile can be obtained conveniently by employing the method proposed in this paper. Although the optimal impedance profile is more complex, it can be effectively realized through precise modifications, such as creating specific patterns of holes in the transmission line plates [2]. Given the substantial investment associated with accelerators and the challenge of enhancing efficiency, the additional complexity in manufacturing the transmission line plates is justified.

IV. CONCLUSION

Through detailed theoretical analysis, it was found that the power transmission efficiency of the NTL is influenced by four factors: the ratio of output impedance to input impedance, the ratio of input pulse width to the NTL's one-way transit time, the normalized impedance profile, and the normalized input pulse. Based on these insights, a method to determine the optimal impedance profile was developed, centered on minimizing the reflection component within the operating frequency range. A case taken from an existing reference demonstrates that, compared to the exponential impedance profile, the optimal impedance profile intentionally reduces high-frequency transmission efficiency to enhance performance at lower frequencies. This trade-off is justified since the input pulse predominantly consists of low-frequency components, resulting in higher power transmission efficiency for the optimal impedance profile.

ACKNOWLEDGMENTS

This work was supported by the National Natural Science Foundation of China under Grant No. 52207181.

APPENDIX A: EXPRESSIONS OF THE OUTPUT COMPONENTS

The reflection coefficient at any point x is determined by Eq. (A1) and the frequency response of the components contributing to the output voltage is presented in Eq. (A2). H_{out0}, H_{out2}, and H_{out4} are the frequency responses of the no-reflection, two-reflection, and four-reflection components, respectively. x_i is the position coordinate where the ith reflection occurs.

Using Eq. (1), Eq. (A2) can be simplified. Taking the H_{out2} as an example, the simplified expression is present in Eq. (A3). The other components can be simplified similarly:

$$\gamma(x) = \frac{Z(x+\mathrm{d}x) - Z(x)}{Z(x+\mathrm{d}x) + Z(x)} = \frac{Z'(x)}{2Z(x)}\mathrm{d}x, \tag{A1}$$

$$\begin{cases} H_{\mathrm{out0}} = \rho_0 \mathrm{e}^{-\mathrm{j}\omega T_{\mathrm{line}}} \\ H_{\mathrm{out2}} = \int_0^L \int_0^{x_1} \rho_0 \frac{Z'(x_1)}{2Z(x_1)} \frac{Z'(x_2)}{2Z(x_2)} \mathrm{e}^{-\mathrm{j}\omega T_{\mathrm{line}}(1+\frac{2(x_1-x_2)}{L})} \mathrm{d}x_1 \mathrm{d}x_2 \\ H_{\mathrm{out4}} = \int_0^L \int_0^{x_1} \int_{x_2}^L \int_0^{x_3} \rho_0 \frac{Z'(x_1)}{2Z(x_1)} \frac{Z'(x_2)}{2Z(x_2)} \frac{Z'(x_3)}{2Z(x_3)} \frac{Z'(x_4)}{2Z(x_4)} \mathrm{e}^{-\mathrm{j}\omega T_{\mathrm{line}}(1+\frac{2(x_1-x_2+x_3-x_4)}{L})} \mathrm{d}x_1 \mathrm{d}x_2 \mathrm{d}x_3 \mathrm{d}x_4, \\ \dots \end{cases} \tag{A2}$$

$$H_{\mathrm{out2}} = \int_0^1 \int_0^{\bar{x}_1} \rho_0 \frac{({\rho_0}^2 - 1)\bar{Z}'(\bar{x}_1)}{2[1 + ({\rho_0}^2 - 1)\bar{Z}(\bar{x}_1)]} \frac{({\rho_0}^2 - 1)\bar{Z}'(\bar{x}_2)}{2[1 + ({\rho_0}^2 - 1)\bar{Z}(\bar{x}_2)]} \mathrm{e}^{-\mathrm{j}\omega T_{\mathrm{line}}(1+2(\bar{x}_1-\bar{x}_2))} \mathrm{d}\bar{x}_1 \mathrm{d}\bar{x}_2. \tag{A3}$$

APPENDIX B: OBJECTIVE FUNCTION AND ITS DIFFERENTIAL EXPRESSION

The constraints between coefficients a_i $(i = 0, 1, 2, ..., k)$ are $Z(0) = Z_{\mathrm{in}}$ and $Z(L) = Z_{\mathrm{out}}$. Combining these two constraints and Eq. (8), it can be found that when a_i $(i = 1, 2, ..., k)$ is determined, the value of a_0 should be

$$a_0 = \frac{1}{2L}\ln\frac{Z_{\mathrm{out}}}{Z_{\mathrm{in}}} - \sum_{n=1}^{k} \frac{a_n}{n+1} L^n. \tag{B1}$$

Using Eq. (B1), the expression of P_{ref1} become Eq. (B2). To minimize P_{ref1}, P_{ref1} performs partial differentiation on each unknown quantity a_i and sets the result to zero. For example, when partially differentiating a_n, we have Eq. (B3):

$$P_{\mathrm{ref1}} = \left(\frac{1}{2L}\ln\frac{Z_{\mathrm{out}}}{Z_{\mathrm{in}}}\right)^2 f(0,0) + \frac{1}{L}\ln\frac{Z_{\mathrm{out}}}{Z_{\mathrm{in}}} a_i \sum_{i=1}^{k}\left[f(0,i) - \frac{L^i}{i+1} f(0,0)\right] + a_i a_j \sum_{i=1}^{k}\sum_{j=1}^{k}\left[\frac{L^{i+j} f(0,0)}{(i+1)(j+1)} - \frac{2L^i}{i+1} f(0,j) + f(i,j)\right], \tag{B2}$$

$$\sum_{i=1}^{k}\left[\frac{2L^{i+n} f(0,0)}{(i+1)(n+1)} - \frac{2L^i}{i+1} f(0,n) - \frac{2L^n}{n+1} f(0,i) + 2f(i,n)\right] a_i + \frac{1}{L}\ln\frac{Z_{\mathrm{out}}}{Z_{\mathrm{in}}}\left(f(0,n) - \frac{L^n}{n+1} f(0,0)\right) = 0. \tag{B3}$$

[1] R. Petr, W. Nunnally, C. Smith Jr., and M. Clark, Investigation of a radial transmission line transformer for high-gradient particle accelerators, Rev. Sci. Instrum. **59**, 132 (1988).

[2] W. A. Stygar, M. Cuneo, D. Headley, H. Ives, R. Leeper, M. Mazarakis, C. Olson, J. Porter, T. Wagoner, and J. Woodworth, Architecture of petawatt-class z-pinch accelerators, Phys. Rev. ST Accel. Beams **10**, 030401 (2007).

[3] C. Mao, F. Sun, C. Xue, N. Ding, D. Xiao, X. Wang, G. Wang, S. Sun, and A. Qiu, Full-circuit simulation of next generation China z-pinch driver CZ30, IEEE Trans. Plasma Sci. **47**, 2910 (2019).

[4] W. Stygar, T. Awe, J. Bailey, N. Bennett, E. Breden, E. Campbell, R. Clark, R. Cooper, M. Cuneo, J. Ennis *et al.*, Conceptual designs of two petawatt-class pulsed-power accelerators for high-energy-density-physics experiments, Phys. Rev. ST Accel. Beams **18**, 110401 (2015).

[5] W. Stygar, W. Fowler, K. LeChien, F. Long, M. Mazarakis, G. McKee, J. McKenney, J. L. Porter, M. Savage, B. Stoltzfus *et al.*, Shaping the output pulse of a

linear-transformer-driver module, Phys. Rev. ST Accel. Beams **12**, 030402 (2009).

[6] D. Sinars, M. Sweeney, C. Alexander, D. Ampleford, T. Ao, J. Apruzese, C. Aragon, D. Armstrong, K. Austin, T. Awe *et al.*, Review of pulsed power-driven high energy density physics research on z at Sandia, Phys. Plasmas **27** (2020).

[7] R. Zhang, C. Mao, K. Huang, X. Zou, and X. Wang, Comparison of nonuniform transmission lines with gaussian and exponential impedance profiles for z-pinch, IEEE Trans. Plasma Sci. **40**, 3395 (2012).

[8] Y. Hu, T. Huang, F. Sun, P. Cong, J. Zeng, X. Zhang, T. Lei *et al.*, Simulation analysis of transmission-line impedance transformers with the Gaussian, exponential, and linear impedance profiles for pulsed-power accelerators, IEEE Trans. Plasma Sci. **39**, 3227 (2011).

[9] D. Welch, T. Genoni, D. Rose, N. Bruner, and W. Stygar, Optimized transmission-line impedance transformers for petawatt-class pulsed-power accelerators, Phys. Rev. ST Accel. Beams **11**, 030401 (2008).

[10] I. A. D. Lewis and F. H. Wells, *Millimicrosecond Pulse Techniques* (Pergamon Press, Oxford, 1959).

[11] C. Mao, X. Zou, and X. Wang, Analytical solution of nonuniform transmission lines for z-pinch, IEEE Trans. Plasma Sci. **42**, 2092 (2014).

[12] Q. Zhou, X. Zou, and B. Qian, Influence of high reflection order components on the transmission characteristics of nonuniform transmission lines, IEEE Trans. Plasma Sci. **51**, 205 (2022).

[13] C. W. Hsue and C. D. Hechtman, Transient analysis of nonuniform, high-pass transmission lines, IEEE Trans. Microwave Theory Tech. **38**, 1023 (1990).

[14] C. W. Hsue, Elimination of ringing signals for a lossless, multiple-section transmission line, IEEE Trans. Microwave Theory Tech. **37**, 1178 (1989).